Image noise sensitivity of dual-energy digital mammography for calcification imaging

Xi Chen [a], Robert M. Nishikawa[b], Suk-tak Chan[c], Lei Zhang[d] , Xuanqin Mou*[a]
[a] Institute of Image Processing & Pattern Recognition, Xi'an Jiaotong University, Xi'an, Shaanxi, 710049, China
[b]Department of Radiology, The University of Chicago, Chicago, Illinois 60637, USA
[c]Department of Health Technology and Informatics, The Hong Kong Polytechnic University, Hung Hom, Hong Kong
[d]Department of Computing, The Hong Kong Polytechnic University, Hung Hom, Hong Kong

ABSTRACT

Dual-energy digital mammography (DEDM) can suppress the contrast between adipose and glandular tissues and generate dual-energy (DE) calcification signals. DE calcification signals are always influenced by many factors. Image noise is one of these factors. In this paper, the sensitivity of DE calcification signal to image noise was analyzed based on DEDM physical model. Image noise levels of two different commercially available digital mammography systems, GE Senographe Essential system and GE Senographe DS system, were measured. The mean noise was about 1.04% for Senographe Essential system, 1.42% for Senographe DS system at 28kVp/50mAs; and was 0.47% for Senographe Essential system, 0.79% for Senographe DS system at 48kVp/12.5mAs. Evaluations were performed by comparing RMS (Root-Mean-Square) of calcification signal fluctuations in background regions and CNR (Contrast-Noise-Ratio) of calcification signals in clusters when these two digital mammography systems were used. The results showed that image noise had a serious impact on DEDM calcification signals. If GE Senographe Essential system was used, calcification signal fluctuations were 200~300μm, and when calcification size is greater than 300μm, the probability of acquiring CNR≥3 is over 50%. If noise reduction techniques are used, the calcification threshold size of CNR≥3 can be lower.

Keywords: dual-energy, digital mammography, image noise, sensitivity analysis

1. INTRODUCTION

Microcalcifications (μCs) are one of the earliest and main indicators of breast cancer. Thus the visualization and detection of μCs in mammography play a crucial role in reducing the rate of mortality of breast cancer. μCs are usually smaller than 1.0 mm and mainly composed of calcium compounds such as apatite, calcium oxalate and calcium carbonate[1]. μCs have greater x-ray attenuation coefficients than the surrounding breast tissues, so they are more visible on homogeneous soft-tissue backgrounds. However, the visualization of μCs could be obscured in mammograms because of overlapping of tissue structures.

Dual-energy digital mammography (DEDM) is considered as a promising technique to improve the detection precision of μCs. In DEDM, low-energy (LE) and high-energy (HE) images of the breast are acquired using two different x-ray spectra. The LE and HE images can be synthesized to suppress the contrast between adipose and glandular tissues of breast, the overlapping breast structures removed, and subsequently the DE calcification image can be generated. However, DEDM can be influenced by many factors in practice, such as x-ray spectra, scatter, image noise, DQE (detection quantum efficiency) of detectors and calibration polynomials.

Investigations have shown DEDM is sensitive to deviations such as scatter and calibration phantom error[2-5]. Image noise, which refers to quantum noise and all kinds of system noise, also has an impact on DE calcification image. It is necessary to analyze the image noise sensitivity of DE calcification signal, which is the basis for evaluating different mammography systems used for DEDM and is useful when comparing different noise reduction algorithms.

*xqmou@mail.xjtu.edu.cn; phone 86 29 8266 3719

Medical Imaging 2011: Physics of Medical Imaging, edited by Norbert J. Pelc, Ehsan Samei, Robert M. Nishikawa,
Proc. of SPIE Vol. 7961, 796155 · © 2011 SPIE · CCC code: 1605-7422/11/$18 · doi: 10.1117/12.877932

In 2002, Lemacks *et al.*[6] gave a calculation model to estimate the quantum noise in DE calcification image under various x-ray spectra, μC size, breast composition and breast thickness, their results were presented in terms of contrast-to-noise-ratio (CNR). Noise reduction techniques[7, 8] have also been investigated to apply to DE imaging. However, in these works, there is a lack of a quantitative analysis of image noise sensitivity, especially the quantitative errors in DEDM introduced by image noise using commercial digital mammography system.

In this paper, we analyzed the sensitivity of DE calcification signal to image noise contained in LE and HE images. Based on the sensitivity formulas, influence of image noise can be evaluated. The noise levels of LE and HE images, acquired from two different commercially available digital mammography systems, were measured. We evaluated the fluctuations and CNR of DE calcification signals when commercial digital mammography systems were used.

2. MATHEMATICAL MODEL AND FORMULA

2.1 Imaging physical model of DEDM

During mammography, the breast is compressed to a uniform thickness T and for this work, the breast is considered to be composed of adipose tissue (thickness t_a), glandular tissue (thickness t_g) and μC (thickness t_c). As the total breast thickness T is automatically measured by x-ray system and the contribution of μC to the total breast thickness can be ignored, the three unknowns t_a, t_g and t_c can be expressed as two unknowns: glandular ratio $g = t_g / T \approx t_g / (t_a + t_g)$ and μC thickness t_c.

The transmitted fluence incident on the detector is given by:

$$P(E) = P_0(E)\exp\left[-\mu_a(E)T - g\left(\mu_g(E) - \mu_a(E)\right)T - \mu_c(E)t_c\right], \tag{1}$$

where $P_0(E)$ and $P(E)$ are the incident photon fluence on the surface of the breast and the transmitted fluence, respectively, $\mu_a(E)$, $\mu_g(E)$ and $\mu_c(E)$ are linear attenuation coefficients of adipose tissue, glandular tissue and μC, respectively.

In DE imaging calculations, a reference signal I_r is needed to change the dynamic range of the intensity values. The exposure data f is defined as the log-value of ratio of the transmitted exposure I to reference signal I_r. The LE and HE logarithmic intensities $f_l(t_c, g)$ and $f_h(t_c, g)$ are measured independently using x-ray beams at different kVps:

$$\begin{aligned} f_j(t_c, g) &= \ln\left(I_{rj} / I_j\right) \\ &= \ln\left(I_{rj}\right) - \ln\left(\int P_{0j}(E)\exp\left[-\mu_a(E)T - g\left(\mu_g(E) - \mu_a(E)\right)T - \mu_c(E)t_c\right]Q(E)\,dE\right), \quad j = l, h. \end{aligned} \tag{2}$$

$Q(E)$ is the detector response.

2.2 Sensitivity formula

In DEDM, the logarithmic intensities f_l and f_h have deviations, including image noise and scatter. In this paper, it is assumed that f_l and f_h are scatter free, since we have proposed a scatter correction method for DEDM[5]. Moreover, we assumed that the reference signals I_{rl} and I_{rh} can be measured with high precision and contribute little noise to f_l and f_h. Therefore, the sensitivities of DE calculation results t_c and g associated with the image noise are represented by $\frac{\partial t_c / t_c}{\partial I_l / I_l}$, $\frac{\partial t_c / t_c}{\partial I_h / I_h}$, $\frac{\partial g / g}{\partial I_l / I_l}$ and $\frac{\partial g / g}{\partial I_h / I_h}$, which are the partial derivatives of t_c and g with respect to transmitted exposures I_l and I_h, respectively. Using differential method of implicit function, the sensitivity formula can be deduced from physical model Eq.(2).

First, we can get:

$$\begin{cases} I_l = \int P_{0l}(E)\exp\left[-\mu_a(E)T - g\left(\mu_g(E)-\mu_a(E)\right)T - \mu_c(E)t_c\right]Q(E)\,dE \\ I_h = \int P_{0h}(E)\exp\left[-\mu_a(E)T - g\left(\mu_g(E)-\mu_a(E)\right)T - \mu_c(E)t_c\right]Q(E)\,dE \end{cases}. \tag{3}$$

Eq.(3) can be transformed to:

$$\begin{cases} J_1 = \int P_{0l}(E)\exp\left[-\mu_a(E)T - g\left(\mu_g(E)-\mu_a(E)\right)T - \mu_c(E)t_c\right]Q(E)\,dE - I_l \equiv 0 \\ J_2 = \int P_{0h}(E)\exp\left[-\mu_a(E)T - g\left(\mu_g(E)-\mu_a(E)\right)T - \mu_c(E)t_c\right]Q(E)\,dE - I_h \equiv 0 \end{cases}. \tag{4}$$

Use differential method of implicit function to calculate the partial derivatives of t_c and g with respect to LE transmitted exposure I_l:

$$\begin{cases} \dfrac{\partial J_1}{\partial I_l} + \dfrac{\partial J_1}{\partial t_c}\times\dfrac{\partial t_c}{\partial I_l} + \dfrac{\partial J_1}{\partial g}\times\dfrac{\partial g}{\partial I_l} = 0 \\ \dfrac{\partial J_2}{\partial I_l} + \dfrac{\partial J_2}{\partial t_c}\times\dfrac{\partial t_c}{\partial I_l} + \dfrac{\partial J_2}{\partial g}\times\dfrac{\partial g}{\partial I_l} = 0 \end{cases} \Rightarrow \begin{cases} -1 + R_c\times\dfrac{\partial t_c}{\partial I_l} + R_g\times\dfrac{\partial g}{\partial I_l} = 0 \\ S_c\times\dfrac{\partial t_c}{\partial I_l} + S_g\times\dfrac{\partial g}{\partial I_l} = 0 \end{cases}, \tag{5}$$

Where

$$R_c = \partial J_1/\partial t_c, R_g = \partial J_1/\partial g, S_c = \partial J_2/\partial t_c, S_g = \partial J_2/\partial g. \tag{6}$$

So

$$\begin{cases} \dfrac{\partial t_c/t_c}{\partial I_l/I_l} = \dfrac{S_g}{R_cS_g - R_gS_c}\times\dfrac{I_l}{t_c} \\ \dfrac{\partial g/g}{\partial I_l/I_l} = \dfrac{-S_c}{R_cS_g - R_gS_c}\times\dfrac{I_l}{g} \end{cases}. \tag{7}$$

Similarity, calculate the partial derivatives of t_c and g with respect to I_h:

$$\begin{cases} \dfrac{\partial t_c/t_c}{\partial I_h/I_h} = \dfrac{-R_g}{R_cS_g - R_gS_c}\times\dfrac{I_h}{t_c} \\ \dfrac{\partial g/g}{\partial I_h/I_h} = \dfrac{R_c}{R_cS_g - R_gS_c}\times\dfrac{I_h}{g} \end{cases}. \tag{8}$$

3. CALCULATION AND EXPERIMENT

3.1 Data for Sensitivity Calculation

Using the formulas derived above, the sensitivity values can be calculated using publicly available data. The imaging conditions agreed with the clinical mammography system. X-ray spectra were 25kVp and 50kVp with Mo anode and 0.03mm Mo filter. The spectra data were obtained from the classical Handbook[9]. The detector consisted of a CsI:Tl converter layer coupled with an aSi:H+TFT flat-panel detector. In our calculation, the scintillator thickness was 45mg/cm^2 for CsI:Tl. All photons transmitted through the imaged object were assumed to be absorbed completely in the perfectly efficient converter layer.

The elemental compositions of glandular and adipose tissue for human breast were from Hammerstein *et al.*[10]. The densities equal to 0.93g/cm^3 for adipose tissue and 1.04g/cm^3 for glandular tissue. Breast thickness was assumed to be

4cm. μCs were assumed to be composed of calcium oxalate (CaC_2O_4). The density is 2.20g/cm^3. Mass attenuation coefficients of different materials were calculated via the database of XCOM from NIST[11].

3.2 Noise Level Measurement of LE and HE Images

The two full-field digital mammography systems used in this study were GE Senographe DS and GE Senographe Essential. The detectors of both systems consisted of a CsI:Tl converter layer coupled with an aSi:H+TFT flat-panel detector. The detector for Senographe Essential system is more advanced and has better image quality. Pixel size was 100μm. Image size was 1914×2294 for Senographe DS system, 3062×2394 for Senographe Essential system. For both systems, two images were output after every exposure, for-processing ("raw") image and processed image. The mammography system automatically used gain nonuniformities, defective pixels, and dark current noise (offset) corrections to every raw image acquired. Raw image is linear. Processed image is logarithmic format, which is the output after the system applied image processing algorithms (denoising, edge enhancement etc.) to raw image. Different processed images have different gray scales, which can't be used for DE calculations. Therefore, raw images were used in our DE experiments.

The total mean-glandular dose and entrance-skin exposure were constrained to typical screening examination levels. 28kVp/50mAs and 48kVp /12.5mAs were used for LE and HE imaging respectively. There were four focal spots in each system, 100μm and 300μm on Mo target, 100μm and 300μm on Rh target. Taking into account the imaging conditions, allowance by the hardware options of system and the possible misregistration if we use two different focal spots for LE and HE imaging, we used the large focal spot (300μm) on the Rh target with the Rh filter in this experiment. The source to image distance was 66cm and the compression plate was removed during image acquisition.

A breast phantom (Fig.1) was used in this experiment. The phantom was a rectangular block with dimension of 12×10×4 cm^3 (length×width×height). This model was a density step phantom that simulated different ratios, 0%, 30%, 45%, 50%, 70% and 100%. The materials of this phantom mimicked the photon attenuation coefficients of a range of breast tissues. The average elemental composition of the human breast being mimicked was based on the individual elemental compositions of adipose and glandular tissues reported by Hammerstein *et al*. [10]

The breast phantom was exposed on both systems. The date of last detector calibration was six months for Senographe DS system, three months for Senographe Essential system before our experiment. The noise level in the LE and HE raw images can be related to the mean value and rms in different regions:

$$\sigma = \text{rms/mean}, \tag{9}$$

where σ, rms and mean are noise level, root-mean-square and mean value of the image region.

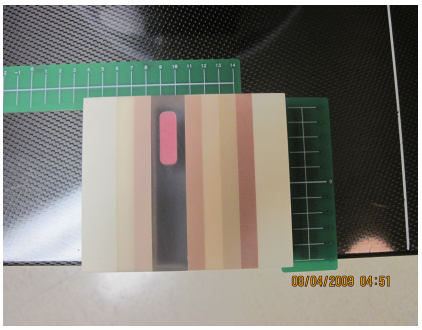

Figure 1. Breast phantom (Model 017, Computerized Imaging Reference Systems Inc., Norfolk, VA, USA).

4. RESULTS AND DISCUSSION

4.1 Sensitivities

Rates of change $\frac{\partial t_c / t_c}{\partial I_l / I_l}$, $\frac{\partial t_c / t_c}{\partial I_h / I_h}$, $\frac{\partial g / g}{\partial I_l / I_l}$ and $\frac{\partial g / g}{\partial I_h / I_h}$, calculated in Eqs.(7) and (8), were used to indicate the sensitivities of DEDM results t_c and g associated with I_l and I_h. In these calculations, the imaged object was human breast and μCs (CaC_2O_4). Data for calculation, such as spectra data, breast composition and detector response function, have been described in section 3.1. Fig.2 illustrates the values of sensitivities when μC thickness 50~500μm and glandular ratio 5%~95%, $\frac{\partial t_c / t_c}{\partial I_l / I_l}$ ranges -463~-25, $\frac{\partial t_c / t_c}{\partial I_h / I_h}$ ranges 1334~105, $\frac{\partial g / g}{\partial I_l / I_l}$ ranges 414~11, and $\frac{\partial g / g}{\partial I_h / I_h}$ ranges -1234~-51. The calculation result t_c and g are very sensitive to image noise, a little noise in the measured I_l and I_h will cause big errors, especially when μC thickness is small.

4.2 Noise Level in LE and HE Images

The breast phantom was exposed on both digital mammography systems at low and high kVps, and noise levels of LE (28kVp/50mAs) and HE (48kVp/12.5mAs) images were evaluated. Regions (50×50 pixel) of different glandular ratios were selected for noise comparison and results are listed in Table 1. It can be seen that the image noises increase with glandular ratio, especially for LE images, since x-ray photon attenuation is more for dense breast at low kVp. At 28kVp/100mAs, the mean noise is about 1.04% for Senographe Essential system, 1.42% for Senographe DS system; at 48kVp/12.5mAs, the mean noise is about 0.47% for Senographe Essential system, 0.79% for Senographe DS system. Image noise of Senographe Essential system is 60%~70% of noise of Senographe DS system.

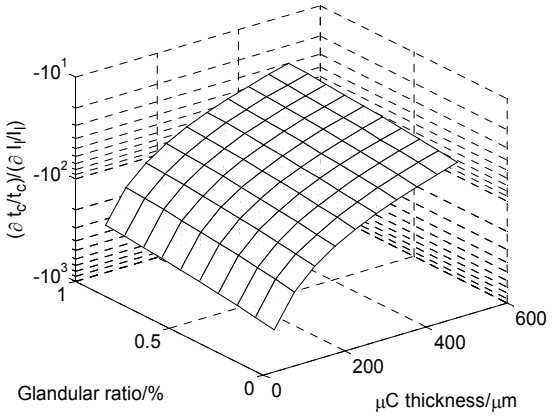

(a) $\frac{\partial t_c / t_c}{\partial I_l / I_l}$

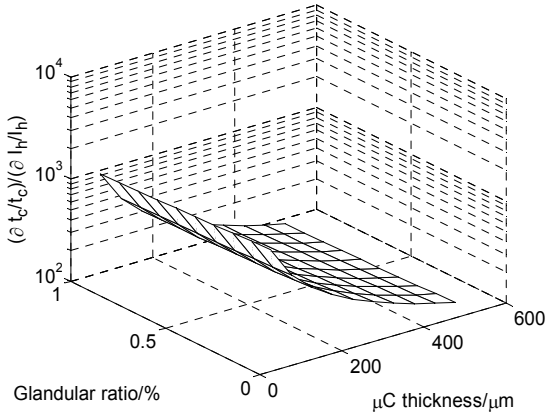

(b) $\frac{\partial t_c / t_c}{\partial I_h / I_h}$

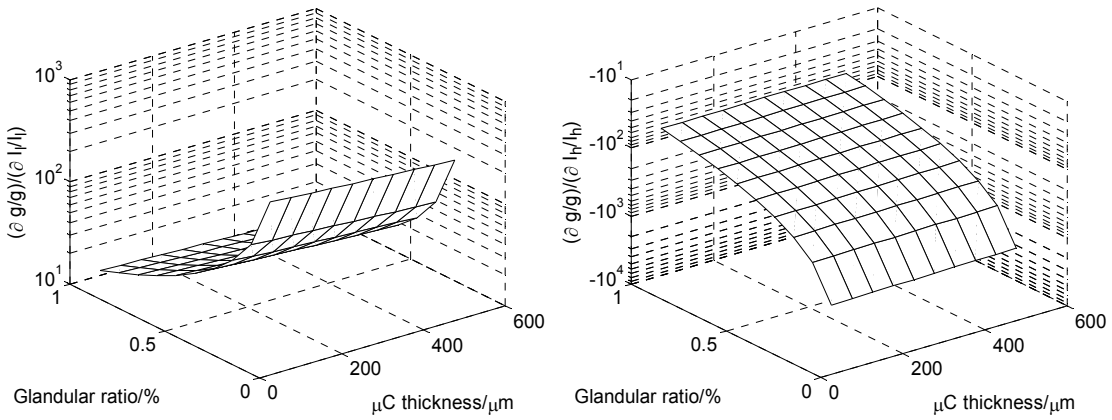

(c) $\dfrac{\partial g / g}{\partial I_l / I_l}$ (d) $\dfrac{\partial g / g}{\partial I_h / I_h}$

Figure 2.Sensitivity values when μC thickness 50~ 500μm and glandular ratio 5%~95%.

Table 1 Image noise of GE Senographe Essential system and GE Senographe DS system

Glandular ratio g (%)	σ(%) of Senographe Essential system		σ(%) of Senographe DS system	
	LE	HE	LE	HE
0	0.85	0.43	1.11	0.70
30	0.88	0.43	1.27	0.70
50	0.98	0.44	1.35	0.76
70	1.15	0.52	1.47	0.80
100	1.32	0.52	1.92	0.97

4.3 Noise level in the calcification image

Taking account of the characteristic of the x-ray detection process, the number of detected photons is a stochastic quantity governed by Poisson statistics. Furthermore, since the number of photons is typically large in diagnostic x-ray imaging, it can be assumed to fluctuate with a Gaussian distribution. Moreover, the image noise are mainly composed of quantum noise, so we assumed that the image noise were Gaussian noise.

According to the noise levels listed in Table 1, noisy LE (25kVp/50mAs) and HE (50kVp/12.5mAs) images (containing Gaussian random noise) were simulated. We assumed the imaged breast consisting of glandular ratios of 0%, 30%, 50%, 70%, 100% and 15 calcification clusters with size of 200, 250, 300μm. Each cluster consisted of 100 μCs with the same size.

Using the noisy LE and HE images, the DE calcification image was generated. The calculated calcification signal in background region, (no μCs present) would be zero if there were no image noise. The minimum, maximum and rms of calcification signal fluctuations introduced by image noise in background region are listed in Table 2.

For each μC, CNR was calculated:

$$CNR = \frac{\left| S_{\mu c} - S_B \right|}{\sigma} \times \sqrt{A} \ , \tag{10}$$

where $S_{\mu c}$ is the DE calcification signal over μC, S_B is the DE calcification signal over background, σ is the noise in S_B and A is the area of μC. For each calcification cluster, the numbers of μCs whose CNR was over 3 or 4 are listed in Tables 3 and 4.

In Table 2, it can be seen that the image noise caused calcification signal fluctuations of 200~300μm for Senographe Essential system, 300~500μm for Senographe DS system. The range of calcification signal fluctuation were about -1300 ~1200μm and -2000~1900μm for Senographe Essential system and Senographe DS system, respectively.

DEDM calculation results were very sensitive to noise in LE and HE images. When glandular ratio is 50% and μC size is 300μm, Table 3 shows that with the Senographe Essential system a CNR of 3 is achieved for 68% μCs; whereas with Senographe DS system, as seen in Table 4, a CNR of 3 is achieved for 39% μCs.

If we use commercially available digital mammography systems for DEDM, the image noise will have a serious impact on results. Although DE imaging could suppress the tissue structures (contrast between adipose and glandular tissues), it also increases the intrinsic noise in the DE calcification images. The main reasons are that approximately half dose of the conventional mammography screening was applied to each image acquisition in DEDM and the image noise in LE and HE images both contribute to the DE calcification image. As can be seen that calcification signal fluctuation increased with glandular ratio, the ability of DEDM to suppress tissue structures was lowered because of image noise. Therefore, it is important to develop denoising algorithms to further improve the diagnostic value of DEDM.

On the other hand, we can just use the raw images for DE calculations. Although the processed images output by the commercial digital mammography systems contain less noise, they have different gray scale, which can't be used for DEDM calculation. If the commercial mammography system can generate denoised images with linear gray scale, by which the DEDM calculation results would be more accurate.

Table 2 Calcification signal fluctuations in DEDM introduced by image noise

Glandular ratio g (%)	Calcification signal fluctuations (μm) in 50×50 pixel region					
	GE Senographe Essential system			GE Senographe DS system		
	min	max	rms	min	max	rms
0	-709	943	224	-949	1156	297
30	-855	742	230	-1096	1157	339
50	-782	956	252	-1184	1355	356
70	-1006	986	296	-1118	1662	399
100	-1285	1194	344	-1947	1883	502

Table 3 Number of μCs (CNR≥3 or 4), GE Senographe Essential system

CNR	μC size (μm)	Glandular Ratio				
		0%	30%	50%	70%	100%
≥3	200	16	8	4	2	0
	250	34	34	23	21	0
	300	76	74	68	57	36
≥4	200	2	1	0	0	0
	250	13	7	4	20	0
	300	55	46	35	24	8

Table 4 Number of μCs (CNR≥3 or 4), GE Senographe DS system

CNR	μC size (μm)	Glandular Ratio				
		0%	30%	50%	70%	100%
≥3	200	7	2	2	0	0
	250	27	14	14	11	2
	300	46	36	39	23	14
≥4	200	0	0	0	0	0
	250	10	4	2	2	0
	300	30	18	16	6	1

5. CONCLUSION

Image noise of two digital mammography systems was evaluated and the sensitivities of DE calculation results to the image noise contained in LE and HE images were investigated. Results showed image noise of GE Senographe Essential system was about 60%~70% of noise of GE Senographe DS system. Image noise has a serious impact on DEDM calcification signals. If GE Senographe Essential system was used, calcification signal fluctuations were 200~300μm, and when μC size is greater than 300μm, the probability of acquiring CNR≥3 is over 50%. If noise reduction techniques are used, the μC threshold size of CNR≥3 can be lower.

ACKNOWLEDGEMENTS

This work was supported in part by grants for the National Science Fund of China (60472004, 60551003), Ministry of Education of China (106143), ICRG of Hong Kong Polytechnic University (YG-79), National Institutes of Health (S10 RR021039), National Institutes of Health / National Cancer Institute (P30 CA14599) and DOD BCRP predoctoral fellowship (W81XWH-080-1-0353). R. M. Nishikawa is a shareholder in and receives royalties from Hologic, Inc. He is a member of the scientific advisory board of Dexela, Ltd. He is a consultant to Siemens Medical Solutions USA and Carestream Health, Inc.

REFERENCES

[1] Fandos-Morera, A., Prats-Esteve, M., Tura-Soteras, JM. and Traveria-Cros, A., " Breast tumors: composition of microcalcifications," Radiology 169(2), 325-327 (1988).
[2] Kappadath, S., Shaw C., "Quantitative evaluation of dual-energy digital mammography for calcification imaging," Physics in Medicine and Biology 49(10), 2563-2576 (2004).
[3] Mou, X., Chen, X., Sun, L., Yu, H., Ji, Z., Zhang, L., "The impact of calibration phantom errors on dual-energy digital mammography," Physics in Medicine and Biology 53(22), 6321-6336 (2008).
[4] Mou, X., Chen, X., "Error analysis of calibration materials on dual-energy mammography," Lecture Notes in Computer Science 4792, 596-603, MICCAI 2007 (2007).
[5] Chen, X., Mou, X., Yan H., "Scatter correction algorithm without extra exposure for dual-energy digital mammography," Proc. SPIE 7258, 725840-1-8 (2009).
[6] Lemacks, M., Kappadath, S., Shaw, C., Liu, X., Whitman, G., "A dual-energy subtraction technique for microcalcification imaging in digital mammography—A signal-to-noise analysis," Medical Physics 29(8), 1739-1751 (2002).
[7] Kappadath, S., Shaw C., "Dual-energy digital mammography for calcification imaging: noise reduction techniques," Physics in Medicine and Biology 53(19), 5421-5443 (2008).
[8] Warp, R, Dobbins Iii J, "Quantitative evaluation of noise reduction strategies in dual-energy imaging," Medical Physics 30(2), 190-198 (2003).
[9] Fewell, T. R., Shuping, R.E., [Handbook of mammographic x-ray spectra], Rockville, USA: HEW Publication (FDA), 59-69 (1978).
[10] Hammerstein, G., Miller, D., White, D., Masterson, M., Woodard, H., Laughlin, J., "Absorbed radiation dose in mammography," Radiology 130(2), 485-491 (1979).
[11] Berger, M., Hubbell, J., Seltzer, S., Chang, J., Coursey, J., Sukumar, R., Zucker, D., "XCOM: Photon cross sections database, NIST standard reference database 8 (XGAM)," http//:www.physics.nist.gov/PhysRefData/Xcom/Text/XCOM.html (2005)